ASTRONOMY & ASTROPHYSICS
SUPPLEMENT SERIES

Astron. Astrophys. Suppl. Ser. **124,** 13-21 (1997)

UBVRI imaging photometry of the open cluster Cr 272[⋆,⋆⋆]

R.A. Vázquez[1], G. Baume[1], A. Feinstein[1] and P. Prado[2]

[1] Observatorio Astronómico de La Plata, Paseo del Bosque s/n, 1900 La Plata and PROFOEG-CONICET, Argentina
[2] University of Toronto Southern Observatory, Las Campanas, Casilla 601, Chile

Received January 10; accepted October 31, 1996

Abstract. We present an extensive CCD *UBVRI* (Cousins system) photometric survey in the region of the open cluster Collinder 272. Our data analysis confirms that the cluster is situated in the outer border of Becker's inner arm -II, at a distance $d = 2300$ pc and probably related to the neighbor cluster Hogg 16. There is no highly evolved stars in the cluster upper sequence and our age estimate based upon isochrones from models computed with mass loss and overshooting, and other methods, indicates a mean age of 13 Myr. A statistical method based on the removal of field stars was used to determine the luminosity function and the initial mass function of the cluster. The cluster initial mass function is characterized by a slope $x = 1.8$.

Key words: cluster: open: individual: Cr 272 — stars: luminosity function, mass function — HR diagram

1. Introduction

The study of young open clusters provides us with a powerful tool to understand how the star formation process is taking place in the Galaxy. Nevertheless, our knowledge on young open cluster systems is far from being complete as most of them are poor groupings composed by a small number of stars with few photometric and spectroscopic measures. Our ongoing program, developed to obtain accurate photometry of this kind of objects, led us to observe Cr 272 in this opportunity.

Collinder 272, C1327−610, ($\alpha_{1950} = 13^{\rm h}27^{\rm m}$, $\delta_{1950} = -61°4'$; $l = 307.62$, $b = +1.25$) belongs exactly to the category of non-studied clusters. It looks like a sparse handful of moderate bright stars projected against a dense star background where no remarkable stellar group suggests us the presence of an open cluster. This fact and the lack of very hot stars have situated this cluster far from the route of the observers. Actually, the only extensive photometric survey belongs to Fenkart et al. (1977) who made observations in the *RGU* passbands confirming that it is a real open cluster. No new attempt to improve our knowledge of Cr 272 neither with photometry nor spectroscopy has been reported.

The aim of our investigation is to re-examine all the cluster parameters (e.g. reddening, distance and age) and determine its luminosity function along with the slope value of its mass function. Section 2 contains a detail of the observations and the reduction procedure. In Sect. 3 we describe the data analysis and Sect. 4 contains the determination of the luminosity and mass functions. Section 5 gives our conclusions.

2. Observations

Five overlapping fields shown in Fig. 1 were measured during two observational runs, on April 1992 and 1994 respectively, in the *UBVRI* Cousins system. However, not all frames could be calibrated in the *I* passband as one night we had no chance of measuring *I* standards; on the other hand, due to an unfortunate telescope pointing, no overlapping is seen in the cluster finding chart (Fig. 2), for $500 < x < 850$ and $900 < y < 1000$. The observations were carried out with the 60 cm telescope of the University of Toronto Southern Observatory equipped with a PM 512×512 Metachrome UV coated chip covering an area of $4'$ on a side (scale is $0.45''$/pixel). Figure 1 reveals that our observations did not cover the whole of the cluster as defined by Fenkart et al. (1977) but a large portion of it.

Although the night 8/9 seemed to be veiled, the mean seeing of the observing runs was $1.3''$. To investigate how the field stars contaminate the cluster area, a comparison frame was taken at 30 arcmin from the center of Cr 272 on May 1995 using the same equipment.

PSF fitting using DAOPHOT (Stetson 1987) running within IRAF was employed to get photometry. Previously, the frames were bias subtracted and flat-fielded. Final

Send offprint requests to: rvazquez@fcaglp.edu.ar

⋆ Based on observations collected at the University of Toronto Southern Observatory, Las Campanas, Chile.

⋆⋆ Table 2 is only available in electronic form at the CDS via anonymous ftp to cdsarc.u-strasbg.fr (130.79.128.5) or via http://cdsweb.u-strasbg.fr/Abstract.html

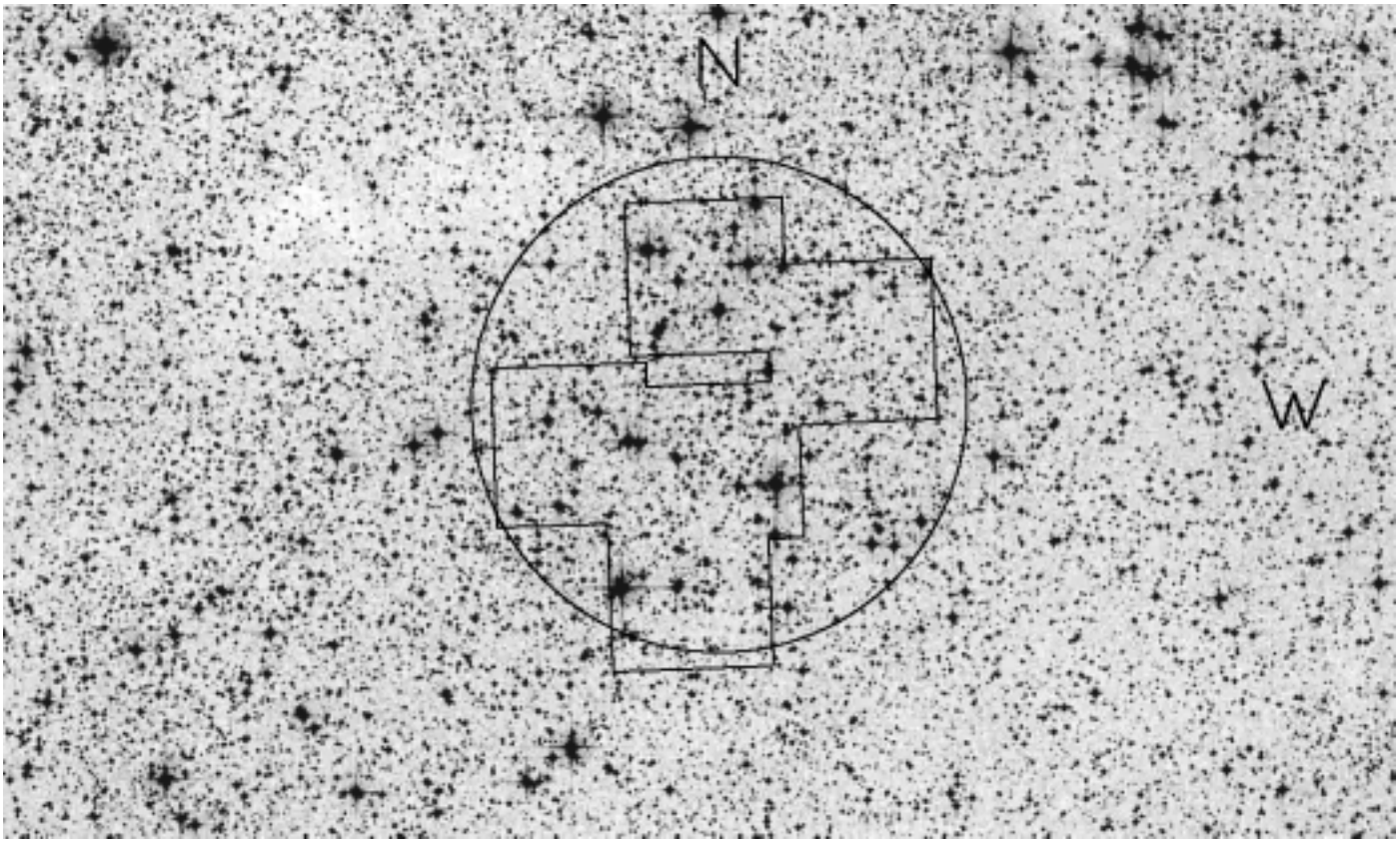

Fig. 1. A reproduction of the **Digitized Sky Survey** plates, **DSS**, showing the area of Cr 272 where the circle gives an estimate of the cluster size, ($\approx 12'$ diameter) calculated from star counts in the **DSS** plates (see Sect. 4). The location of our five frames is also shown. North is at top

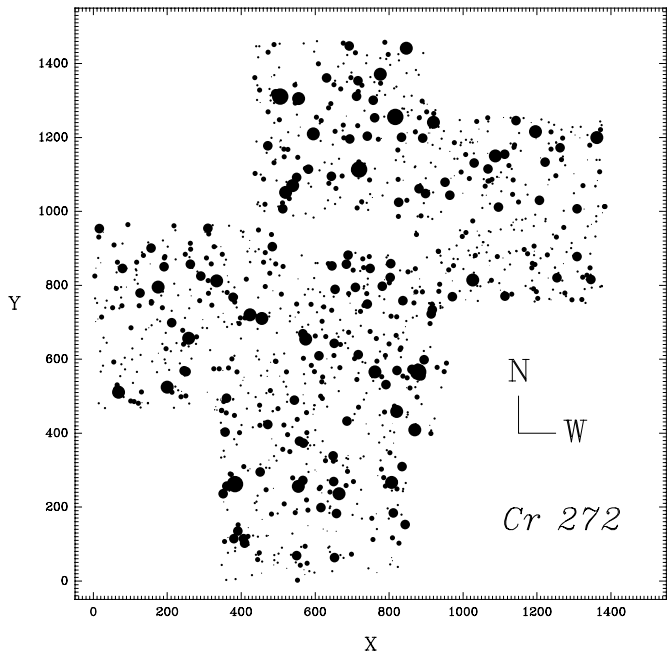

Fig. 2. The finding chart of Cr 272. The size of the dots is proportional to the star magnitudes, approximately

colors and magnitudes were obtained using two well defined sequences in the clusters NGC 5606 and Hogg 16 (Vázquez & Feinstein 1991a,b) as secondary calibration standards. Most of the calculations were carried out at the Observatory of La Plata but a part of them was preliminary made at the Astronomical Institutes of Bonn University. The rms of the transformation equations have been of the order of 0.01 to 0.02, except in the night 8/9 where the rms reaches up to 0.06. Details of exposure times per filter and night can be found in Table 1.

Table 2 lists 1201 stars with available CCD data containing the identification numbers in Col. 1, x and y coordinates in the second and third columns respectively and magnitudes and colors in the remaining columns. The accuracy of CCD data is given in Figs. 3a-e where color and magnitude photometric errors from DAOPHOT are plotted against V.

3. Data analysis

3.1. Memberships

Photometric diagrams of observed data are shown in Figs. 4 to 6. In particular, the two-color diagram, reveals a cluster sequence clearly outlined up to $B-V \approx 0.70$ but

Table 1. Exposure times in Cr 272

Filter	*Exposure*	1992 (April)				1994 (April)
		5/6/7	8/9	9/10	11/12	12/13
U	long	3×900	3×900	2×900	3×900	2×1200
	medium				2×400	
	short		2×400	2×450	1×200	
B	long	4×320	2×400	2×400	3×600	2×700
	medium				2×180	
	short	2×160	2×200	2×200	2×60	
V	long	2×320	2×320	2×250	2×320	2×450
	medium				2×180	
	short	2×40	2×100	2×100	1×25	1×150
R	long	2×100		2×100	2×120	2×110
	medium	2×20			2×50	
	short	2×10		2×50	1×15	1×50
I	long	2×60		2×100	2×100	2×110
	medium			2×30	2×50	1×20
	short	2×16		2×10	1×15	1×5

Note: The columns give the *number of combined frames* $\times$ *exposure time* [*sec*].

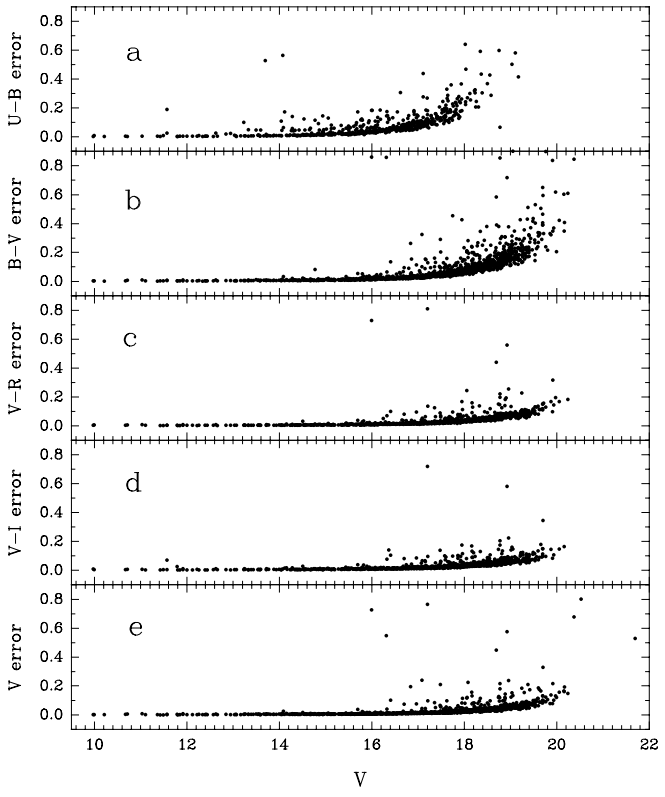

Fig. 3. a-e). The color and magnitude errors from DAOPHOT as a function of the V magnitude

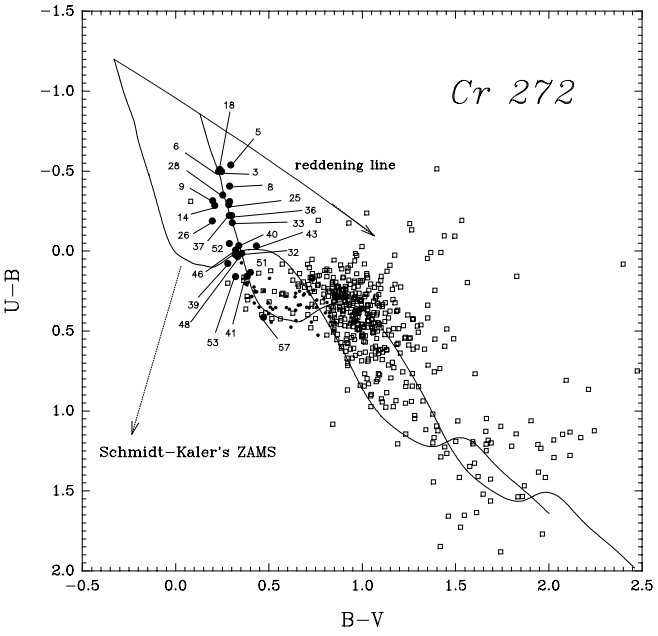

Fig. 4. The two-color diagram of Cr 272. Big dots denote likely cluster members. Small dots are probable members found by comparison among the photometric diagrams. Squares are stars for which no realistic memberships could be determined. The solid line is the Schmidt-Kaler (1982) ZAMS of stars of luminosity class V and the path of the reddening line $E_{U-B}/E_{B-V} = 0.72 + 0.05 \times E_{B-V}$ is indicated with an arrow. Numbers give the star identification

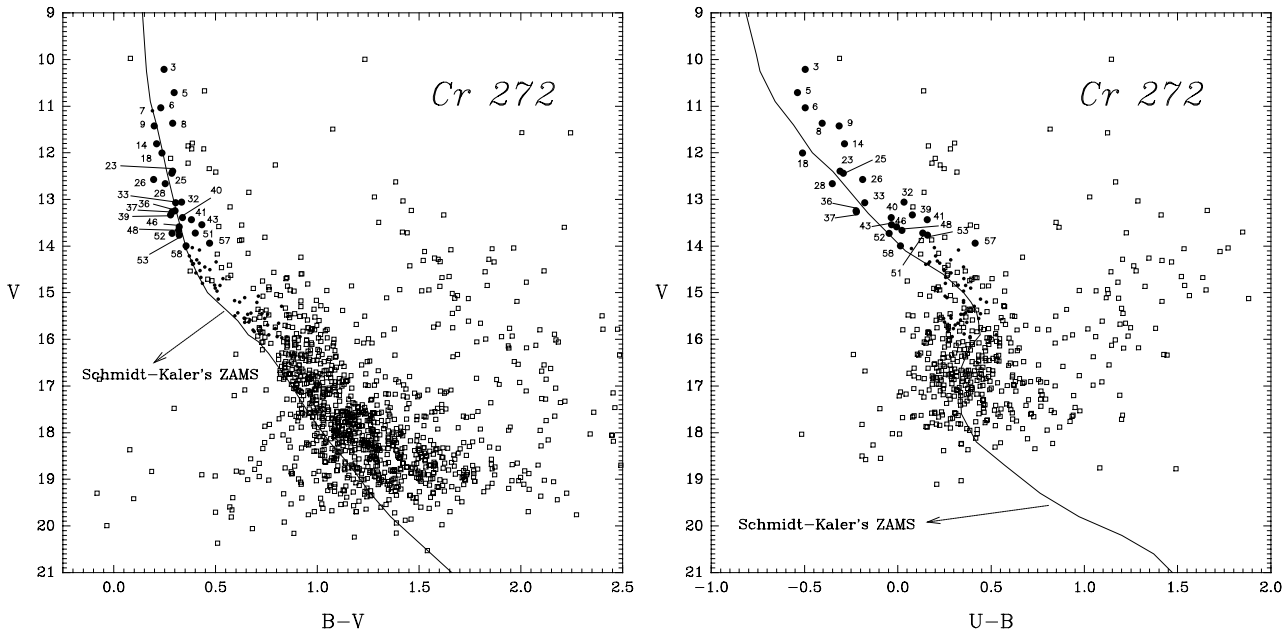

Fig. 5. a) The V vs. $B-V$ color-magnitude diagram. The Schmidt-Kaler (1982) Zams is superposed according to the distance modulus obtained in Sect. 3.2. Symbols as in Fig. 4. **b)** The V vs. $U-B$ color-magnitude diagram. Symbols as in Fig. 4

merging into field stars for larger values of $B-V$. The slight spread shown by the bluest stars in this diagram could be due to differential reddening as photometric errors or contamination by neighbors can be discarded. Also in this diagram, many heavily reddened blue stars are located above the reddening line suggesting, in principle, the presence of absorbing material behind the cluster. However, since some of them have large $U-B$ errors (> 0.08 mag) their settlements in this diagram are definitely dubious and no firm conclusion can be drawn.

After inspecting all the photometric diagrams, membership assessment could be done realistically for stars down to $V \approx 16$ mag. By comparison, mainly in the *UBV* diagrams, a total of 26 likely members were found down to $V \approx 14$ along with several probable members contained in the range $10 \leq V \leq 16$. All likely members have single reddening solution in the $U-B, B-V$ diagram and, by assuming that they are all of luminosity class V, reddening-free *UBV* colors were obtained by a standard procedure (Vázquez et al. 1994) where individual determinations of color excesses yielded mean reddenings $\langle E_{B-V}\rangle = 0.45 \pm 0.06$ and $\langle E_{U-B}\rangle = 0.33 \pm 0.04$ respectively. Probable members found for $B-V \geq 0.70$ and $V < 16$ mag were all de-reddened with the mean color excesses derived from likely members.

The brightest stars of the cluster, #3, 5, 6 and 8, show changing positions in the photometric diagrams: they are all shifted to the right side in the V, $B-V$ diagram while in the V, $U-B$, in addition to them, we found that #9 and 14 show an extra-displacement too. Besides, in the V, $V-I$ array, where there is no $V-I$ index of star #3, we notice that stars #5 and 6 are also at the right side of the main sequence band. This fact could be explained by a variety of causes such as weak emission of B-type stars, unresolved companions, binarity, and, finally, Ap stars, any of them causing the stars to move from their positions in the main sequence band. Another stars, as #18, 28, 36 and 37 appear, however, subluminous (chiefly in the V, $U-B$ diagram) whereas stars #9, 14, 26, 39 and 53 are less affected by reddening.

Considering only the bright stars, the reddening increases from east to west and from south to north across the cluster following the noticeable dust distribution in Fig. 1 although it never surpasses a total variation of 0.30 mag.

Nonetheless, looking at Fig. 6b another peculiarity emerges: most of likely members are placed between R-values from 3.1 to even larger than 3.6. Are these anomalous R-values produced by the interstellar material in the cluster environment?

When we investigated the neighbor cluster Hogg 16 (Vázquez & Feinstein 1991b), situated at 16′ of Cr 272, we found a normal value $R = 3.0$ and a similar mean reddening $\langle E_{B-V}\rangle = 0.44$. Therefore, it is not simple to think of a mechanism able to change suddenly the interstellar matter properties in a so small and trivial region. Indeed, spectroscopy and polarimetry of the bright members could help us to explain their peculiar R-values and red displacements.

Meanwhile, we will adopt a normal value $R = 3.1$ to produce reddening-free magnitudes in the $V_0, (B-V)_0$ diagram of Fig. 7 as $V_0 = V - 3.1 \times E_{B-V}$.

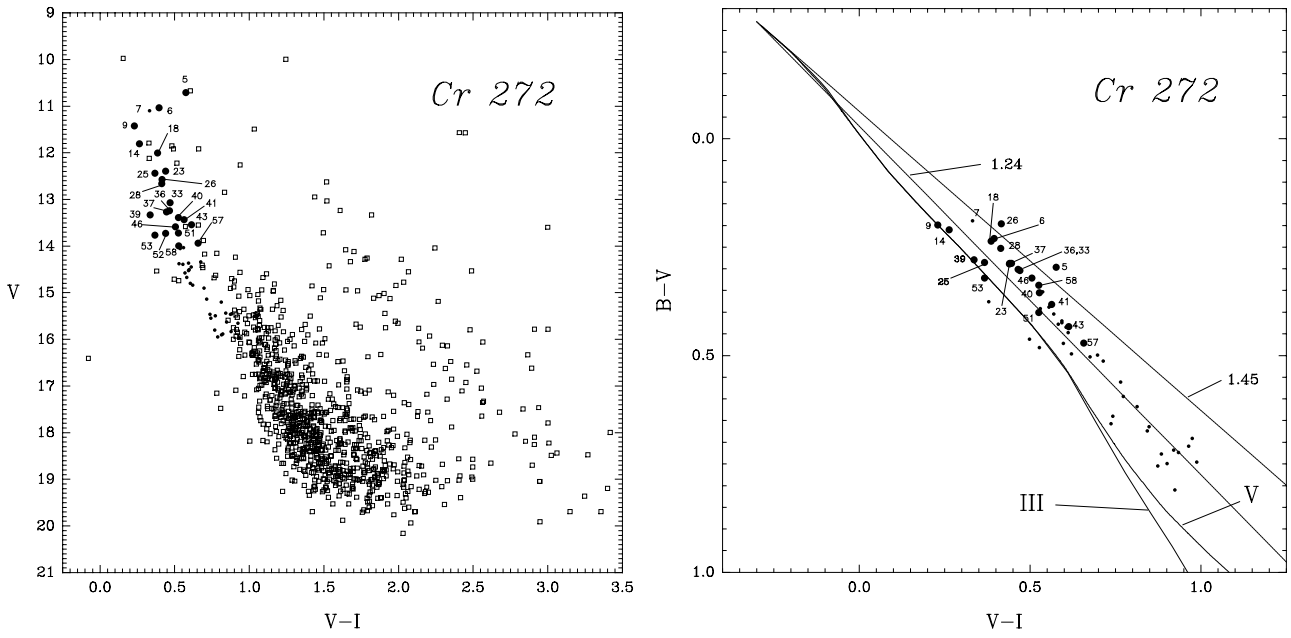

Fig. 6. a) The V vs. $V-I$ color-magnitude diagram. Symbols as in Fig. 4. **b)** The $B-V$ vs. $V-I$ diagram. Solid lines indicate the intrinsic colors for stars of luminosities V and III according to Cousins (1978). The dotted lines show the path of the reddening with slopes 1.24 ($R=3.1$) (Dean et al. 1978) and 1.45 ($R=3.6$) respectively Symbols as in Fig. 4

3.2. Distance and age

The superposition of the ZAMS (Schmidt-Kaler 1982) in the corrected diagram of Fig. 7 gives a distance modulus $V_0 - M_V = 11.84 \pm 0.15$ that situates the cluster at $d = 2300 \pm 200$ pc from the Sun and close to the outer border of the Becker's inner arm-II, as suggested by Fenkart et al. (1977). The latter authors found a cluster distance of $d = 2800$ pc, the difference with ours being produced, mainly, by the uncertainty of the ZAMS fitting in the scattered cluster sequence obtained by them. If instead of $R = 3.1$ we had used $R = 3.4$ (an average of Fig. 6b), the distance of Cr 272 would have been $d = 3200$ and our conclusions would not change at all.

With the cluster distance modulus we obtained the M_V mag of the likely members listed in Table 3 together with their intrinsic colors and excesses. We also show in the table the "equivalent" spectral types based upon the Schmidt-Kaler (1982) calibration. The cluster earliest spectral type could be situated between "b1" and "b2", later than "o5" proposed by Fenkart et al. (1977).

By fitting the isochrones of Maeder & Meynet (1988) evolutionary models to the cluster upper sequence of Fig. 7, we found a cluster age of 15.8 Myr. As this fitting is somewhat uncertain, we inspected other possibilities such as the bluest color at the turnoff point (in $(B-V)_0 = -0.27$) which gives an age of 10 Myr according to the calibration of Meynet et al. (1993), on a side. Also, by interpolation in Maeder & Meynet models, the actual mass of the most luminous star, #3, is 10.4 $\mathcal{M}_\odot$ corresponding to an age of 14.3 Myr. Nevertheless, star #5, situated close to the ZAMS, has a mass of 11.6 $\mathcal{M}_\odot$ and its age is then 12.5 Myr. Therefore, we adopt 13 ± 1 Myr as a reasonable estimate of the cluster age.

Among the stars observed by Vázquez & Feinstein (1991b) in Hogg 16, four of them lie in the field of Cr 272. In particular, stars #53 and 71 in that paper (#6 and 18 in the present work, respectively) are, indeed, members of Cr 272 and not of Hogg 16.

The angular distance between Cr 272 and Hogg 16 is only 16′ ($\approx$ 10 pc) and Hogg 16 is, in addition, $\approx 23 - 26$ 10^6 yr old, as seen in Fig. 7. Therefore, considering that, at 1σ level these clusters are at a same distance from the Sun and have similar reddenings, they could represent an example of sequential formation (Elmegreen & Lada 1977) where the bright stars of Hogg 16 triggered the star formation in Cr 272. Recently, Subramaniam et al. (1995) proposed that about 8% of the known galactic clusters could be members of binary systems. In this hypothetical case, we mention that Cr 272 and Hogg 16 have linear separation and age difference of the order of typical pairs listed by those authors.

As already noticed by Fenkart et al. (1977) no evolved stars are found in the cluster. Looking for them in the periphery of Cr 272, we found the star HD 117399, a δ Cep V659 Cen variable with spectral type F6/7Ib and period $P = 5^{\rm d}.621605$ (Houk & Cowley 1975), situated at $\approx 20'$ to the southwest. This star has no chance to be a cluster member because Evans (1992) and also Fernie et al. (1995) indicate that it has $\langle M_V \rangle = -3.2$ and a companion star of

Table 3. The likely cluster members of Cr 272

#	*F*	$(B-V)_0$	E_{B-V}	$(U-B)_0$	E_{U-B}	*Phot.ST*	V_0	M_V	*Rem*
3		−0.24	0.48	−0.86	0.36	b2iv	8.70	−3.13	
5	15	−0.27	0.56	−0.96	0.42	b1.5v	8.95	−2.88	(1)
6	10	−0.23	0.46	−0.84	0.34	b2v	9.60	−2.24	(2)
8	70	−0.22	0.51	−0.78	0.38	b2.5v	9.79	−2.05	
9	50	−0.17	0.37	−0.59	0.28	b5v	10.27	−1.57	
14	45	−0.17	0.38	−0.56	0.28	b5v	10.64	−1.20	
18	103	−0.24	0.48	−0.87	0.36	b3v	10.52	−1.32	(3)
23	11	−0.19	0.48	−0.67	0.36	b3.5v	10.89	−0.95	
25		−0.19	0.47	−0.64	0.35	b5v	10.97	−0.87	
26		−0.13	0.33	−0.43	0.24	b7.5v	11.55	−0.29	
28		−0.20	0.45	−0.69	0.34	b4v	11.26	−0.58	(3)
32		−0.10	0.43	−0.28	0.32	b8.5v	11.73	−0.11	
33		−0.15	0.46	−0.52	0.34	b6.5v	11.65	−0.19	
36	101	−0.17	0.47	−0.57	0.35	b6v	11.79	−0.05	(3)
37	100	−0.17	0.45	−0.56	0.34	b6v	11.86	0.02	(3)
39	35	−0.07	0.35	−0.18	0.26	b9/a0v	12.25	0.41	
40		−0.12	0.46	−0.37	0.34	b8/b9v	11.98	0.14	
41		−0.07	0.45	−0.18	0.34	b9/a0v	12.03	0.19	
43		−0.14	0.57	−0.46	0.43	b7/b8v	11.76	−0.08	
46		−0.11	0.43	−0.32	0.32	b9/a0v	12.26	0.42	
48	65	−0.10	0.42	−0.29	0.31	b8/b9v	12.37	0.53	
51		−0.08	0.48	−0.22	0.36	b9v	12.23	0.39	
52		−0.11	0.40	−0.34	0.29	b8.5v	12.50	0.66	
53	43	−0.05	0.38	−0.12	0.28	b9.5v	12.60	0.76	(2)
57		0.01	0.46	0.07	0.34	a0v	12.51	0.67	
58	97	−0.11	0.46	−0.33	0.34	b8.5v	12.56	0.72	

Note: The first column contains the star identification numbers used in this work and the second one contains the numbers from Fenkart et al. (1977). The spectral types shown in Col. 7 were derived from a combination of intrinsic indices and the resulting M_V adopting the calibrations given in Schmidt-Kaler (1982).

Rem: (1), not measure available in Fenkart et al.; (2), non member according to Fenkart et al.; (3), slightly underluminous according to their intrinsic color indices.

spectral type B6. Therefore, it does not fit into the scheme of Cr 272 as seen in Fig. 7.

4. Estimation of the cluster luminosity function. The initial mass function

4.1. The luminosity function **LF**

In view of the contamination of field stars for $V \geq 15.5$ mag, we applied a statistical treatment of data to estimate the cluster **LF**. The method relies upon the removal of field stars in the V, $B-V$ diagram of Fig. 5a. To carry out the procedure a comparison area was measured at $30'$ from Cr 272 which V, $B-V$ diagram is shown in Fig. 8. The lack of a fast routine precluded us to assess the completeness of our photometry; however, star counts per magnitude bins shown in Table 4 are indicating that in the cluster and the comparison field, the completeness is quite similar. Anyway, we are confident that down to $V \approx 17$ mag (three magnitudes above the detection limit) the completeness should be reasonably acceptable.

Before removing stars, the comparison field counts were increased by a factor of 4.5 to compensate the different sizes of the areas we measured. Figures 5a and 8 were subdivided into bins of size $\Delta V = 1.0$ mag and $\Delta(B-V) = 0.25$ mag. In particular, the counts per bins of Fig. 8 were smoothed by means of the product of a marginal distribution $\mathcal{F}(V)$ and a relative distribution $\mathcal{G}(B-V/V)$; in this way, we obtained expected field counts which were then subtracted bin per bin from Fig. 5a. With the left counts we constructed the V distribution of statistical cluster members.

This distribution is still affected by photometric errors based upon Poisson statistics of counts in a digital aperture which, as shown in Fig. 3, increase at faint magnitudes, and by photometric uncertainties of the transformation equations and the internal photometric errors (altogether $\sigma_V < 0.08$). After reducing the counts in each

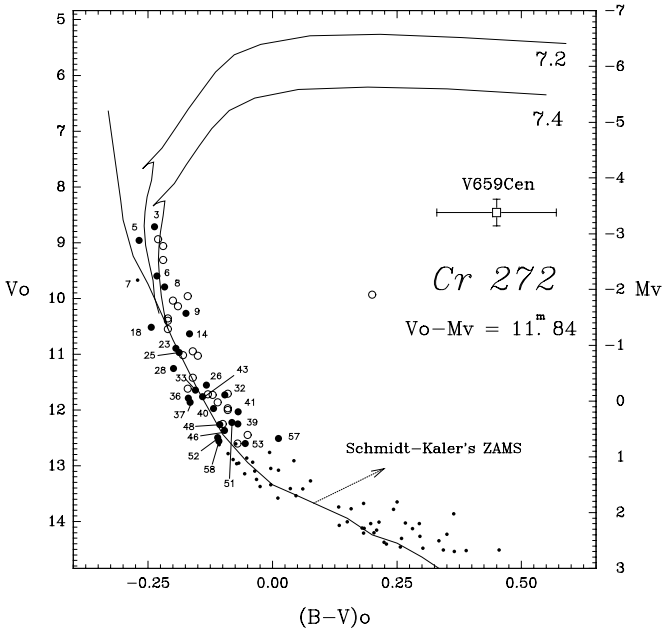

Fig. 7. The V_0 vs. $(B-V)_0$ diagram. Symbols as in Fig. 4. The Schmidt-Kaler ZAMS (1982) and the isochrones (Maeder & Meynet 1988) are superposed. Numbers above the isochrones are the log of age. The vertical right axis shows the M_V scale. The cross is indicating the position of star V659 Cen from Fernie et al. (1995) data. Open circles are the brightest stars of the neighbor open cluster Hogg 16 (Vázquez & Feinstein 1991b)

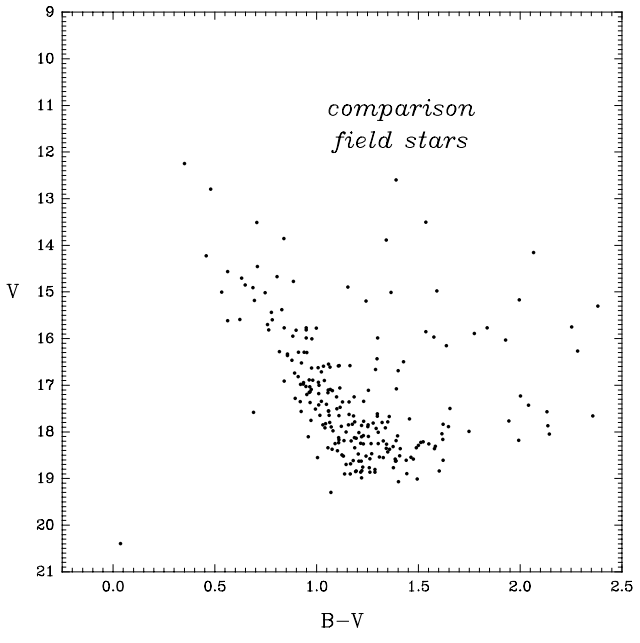

Fig. 8. The V vs. $B-V$ diagram of field stars

Table 4. Stellar counts by ΔV in Cr 272 and comparison field

ΔV	$N_{\rm cluster}$	$N_{\rm field}$
9-10	2	-
10-11	3	-
11-12	12	-
12-13	13	3
13-14	28	4
14-15	67	11
15-16	116	27
16-17	186	35
17-18	282	72
18-19	354	80
19-20	127	3
20-21	8	2
21-22	2	-
22-23	1	-

Note: The column containing the counts of field stars is not scaled (see text).

bin to the central frequencies we estimated that the influence of all these errors together causes the counts in each bin to be decreased by less than 4% in relation to the original ones. The final impact of these errors on the **LF** estimate is however negligible when comparing to the Poisson errors of the counts in every bin that were between $10-20$ times larger. After all these corrections we obtained the cluster **LF** shown in Col. 5 of Table 5.

Is this **LF** representative of the whole cluster **LF**? To answer this we used the **Digitized Sky Survey** plates, **DSS**, to compute the apparent size of the cluster (shown by the circle in Fig. 1) firstly. We started by counting stars in a large area including Cr 272. Taking concentric annuli around a centroid (determined with the bright cluster members) we found that at $6'$ from it the cluster stellar density merges into the general stellar field density. Thus, we adopted $12'$ as the cluster size.

Our second step was to re-calibrate the star magnitudes obtained from the **DSS** plates using a CCD photometric sequence in Cr 272. In this way we produced a set of $V_{\rm DSS}$ magnitudes with a detection limit around $V_{\rm DSS} \approx 18$ and typical errors of 0.5 mag. We had to deal, however, with some blended and/or saturated stars uniformly distributed across the plate. Next, the sample was subdivided into two groups shown in Fig. 9a: the first one contains **all** DSS stars found within the cluster boundaries (the circle of Fig. 1) while the second is composed by only those stars found in the whole area covered by our survey. If we assume that the cluster members are similarly distributed in the two samples we would not expect to find any significant difference between them. These two samples were then compared by means of a χ^2 test, which demonstrated that they are the same with more than 90% reliability, at

Table 5. The **LF** and the initial mass function of Cr 272

ΔV	ΔM_V	$\log \overline{\mathcal{M}}$	$\Delta \log \overline{\mathcal{M}}$	N	$\log \frac{N}{\Delta \log \mathcal{M}}$
10-11	−3.2, −2.2	1.026	0.180	2	1.05
11-12	−2.2, −1.2	0.846	0.180	5	1.44
12-13	−1.2, −0.2	0.666	0.180	5	1.44
13-14	−0.2, 0.8	0.502	0.148	15	2.01
14-15	0.8, 1.8	0.362	0.132	16	2.08
15-16	1.8, 2.8	0.239	0.114	45	2.60
16-17	2.8, 3.8	0.135	0.094	39	2.62
17-18	3.8, 4.8	0.047	0.082	33	2.60
					x = 1.81
					Se = 0.18
					R = 0.95

Note: The first and second column contain the V and M_V ranges whithin which the counts of Col. 5 were performed. Columns 3 is the log of the stellar mass according to Scalo (1986) and Col. 4 is the mass logarithm difference. Column 6 is the IMF obtained with a least squares fitting where data of the last bin $\Delta V = 17 - 18$ were not taken into account. The parameters of the least squares method, the fitting slope "x", the slope error "Se" and the regression coefficient "R" are given in the bottom of the table.

least down to $V \approx 16.5$. Therefore, the χ^2 secures that our estimate of the **LF** shown in Table 5, performed in the area covered by our five frames, represents the whole cluster **LF**.

4.2. The initial mass function (IMF)

We derived the initial mass function from the cluster **LF** through a known mass-luminosity relation. To compute the slope of the mass function we performed a least squares fitting using the expression $\log(N/\Delta(\log\mathcal{M}))= -x \log \mathcal{M}$.

We adopted the mass-luminosity relation found by Scalo (1986), shown in columns two and three of Table 5; but, previously we compared it to a mass-luminosity relation derived from Schmidt-Kaler (1982) data. We found a reasonable agreement between the latter and Scalo's with typical differences in $\log \mathcal{M}$ and, consequently, in $\Delta \log \mathcal{M}$ of −0.018 and 0.008 respectively when $\mathcal{M} < 10.5\ \mathcal{M}_\odot$. Any of these two mass-luminosity relations leads therefore to slope-values differing by no more than a few hundredths.

To avoid incompleteness effects in the determination of the IMF slope we just considered the range $1.3 < \mathcal{M} < 10.5\ \mathcal{M}_\odot$, this is from $V = 10$ to $V = 16.5$ mag where we have maximum certainty on statistical memberships and photometric completeness. Table 5 includes in the last column the value $\log(\Delta N/\Delta(\log\mathcal{M}))$ derived from the **LF** together with the corresponding slope value, $x = 1.8$.

The cluster IMF is graphically shown in Fig. 9b. At 1σ level, it is steeper than the corresponding to a Salpeter (1955) law with $x = 1.35$ and just at 2σ level there is a weak approximation to a Salpeter law. When it is compared to average slopes obtained for groups of open clusters of distinct ages (Tarrab 1982), it is also steeper than the expected for clusters of 13 My (from $x = 0.3$ to $x = 1.5$) and even a bit more than the resulting average slope of "composite" cluster IMFs ($\langle x \rangle = 1.7$). We want to mention that, on the other hand, the slope of the IMF of Cr 272 resembles typical slope-values mainly found in the outer galaxy field (Conti 1992).

5. Conclusions

Cr 272 is a 13 Myr open cluster situated at a distance of 2300 pc from the Sun, close to the outer border of the inner arm -II. It is a spiral arm-tracer seen projected against a dusty region as it has been already stated by Fenkart et al. (1977). Indeed, further observation, e.g. polarimetry and spectroscopy, are needed to explain anomalous R-values. While the material in the direction to the cluster has a low chance of being responsible of this feature (which is confirmed by the normal reddening law in the neighbor cluster Hogg 16), we think that real star-to-star variations of R could be happening in the cluster itself.

Our analysis indicates that the cluster IMF is characterized by a slope $x = 1.8$ that, even at 2σ level, is still a bit far from reconciliating a typical Salpeter slope. Concerning the membership analysis (enterely based on photometric arguments), the reliability of the slope of Cr 272 appears to be out of discussion due to the conservative mass interval we have adopted to minimize incompleteness effects. Although this slope could change (but not dramatically) if another field star sample is considered, we should recall, however, that only proper motion and radial velocity studies can produce a more reliable result.

In view of the similar distances ($\approx$ 2300 pc), proximity to each other ($16'$ or $\approx$ 10 pc), similar reddening values ($\approx$ 0.44) and the age difference ($\approx$ 10 Myr) there is a chance for Cr 272 and Hogg 16 to be evolutionary linked.

This article is partially based on photographic data obtained using the UK Schmidt Telescope operated by the Royal Observatory Edinburgh. Original plate material is copyright the Royal Observatory Edinburgh and the Anglo-Australian Observatory. The plates were processed into the compressed digital form with their permission. The **Digitized Sky Survey** *was produced at the Space Telescope Science Institute under US Government grant NAG W-2166.*

Acknowledgements. The authors are indebted to Dr Garrison for the allocation of telescope time. R.A.V. thanks the generous collaboration of the Astronomical Institute of Bonn (Germany) staff during a scientific visit in 1992 granted by the Deutscher

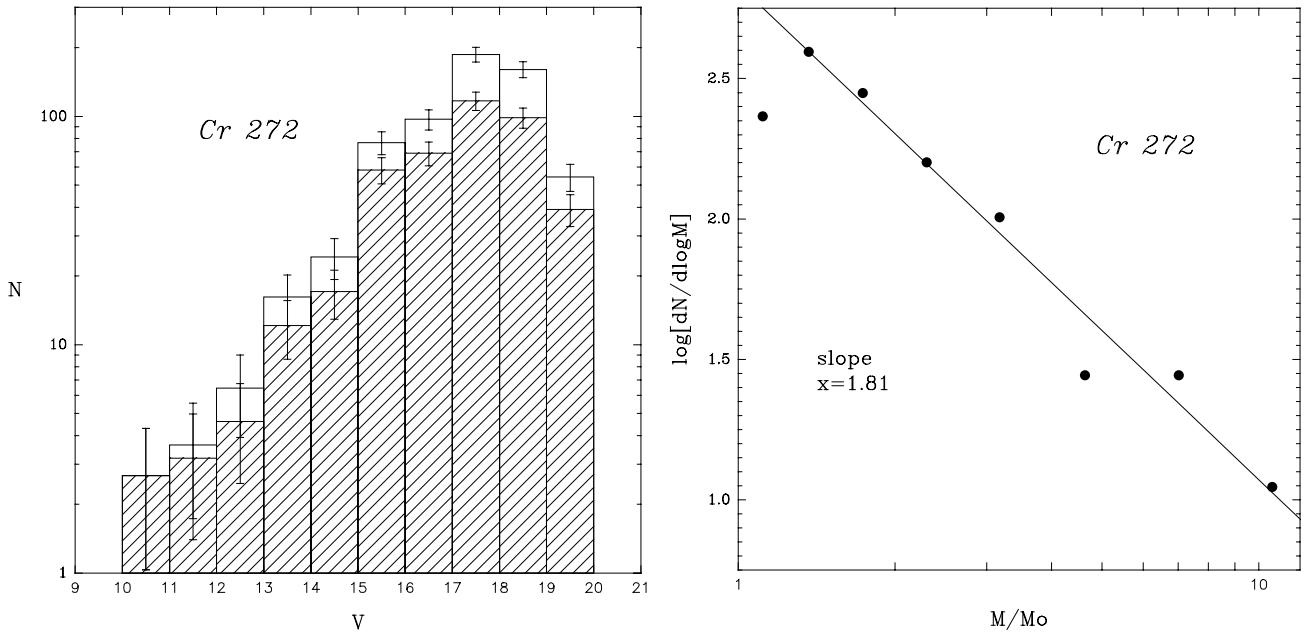

Fig. 9. a) The $V_{\rm DSS}$ mag distribution computed with **all** stars detected in the **DSS** plate within the circle in Fig. 1 (clean histogram) and with the stars detected in the zone covered by the five frames (dashed histogram). The vertical scale is logarithmic and the bars are the Poisson errors. **b)** The IMF of Cr 272. The solid line (slope 1.8) is the least squares fitting in which computation the less massive point was not taken into account

Akademischer Austauschdienst and the CONICET. We also acknowledge the comments and suggestions to improve this article made by Dr. J.-C. Mermilliod.

References

Conti P.S., 1992, in IAU Symposium 149, The Stellar Population of Galaxies, Barbuy B. and Renzini A. (eds.), p. 93
Cousins A.W.J., 1978, Mon. Not. R. Astron. Soc. S. Afr. 37, 62
Dean J.F., Warren P.R., Cousins A.W.J., 1978, MNRAS 183, 569
Elmegreen B.G., Lada C.J., 1977, ApJ 214, 725
Evans N.R., 1992, ApJ 389, 657
Fenkart R.P., Binggeli B., Good D., Jenni D., Labhardt L., Tschumi A., 1977, A&AS 30, 307
Fernie J.D., Beattie B., Evans N.R., Seager S., 1995, in "A data base of galactic classical cepheids", a machine readable catalogue
Houk N., Cowley P.A., 1975, The University of Michigan Catalogue of two dimensional Spectral types for HD stars, Department of Astronomy, Univ. of Michigan
Maeder A., Meynet G., 1988, A&AS 76, 411
Meynet G., Mermilliod J.-C., Maeder A., 1993, A&AS 98, 477
Scalo J.M., 1986, Fund. Cos. Phys. 11, 1
Salpeter E.E., 1955, ApJ 121, 161
Schmidt-Kaler Th., 1982, in Landolt-Bornstein VI/2b
Stetson P.B., 1987, PASP 99, 191
Subramaniam A., Gorti U., Sagar R., Bhatt H.C., 1995, A&A 302, 86
Tarrab, I., 1982, A&A 109, 285
Vázquez R.A., Baume G., Feinstein A., Prado P., 1994, A&AS 106, 339
Vázquez R.A., Feinstein A., 1991a, A&AS 87, 383
Vázquez R.A., Feinstein A., 1991b, A&AS 90, 317